PL-TR-93-2263

AD-A278 563

A STUDY OF THE IMPACT OF CIRRUS CLOUDS ON HIGH ALTITUDE, LONG HORIZONTAL PATH LASER TRANSMISSION

G. G. Koenig
D. R. Longtin
J. R. Hummel

SPARTA, Inc.
24 Hartwell Avenue
Lexington, MA 02173

23 December 1993

Scientific Report No. 7

94-08766

PHILLIPS LABORATORY
Directorate of Geophysics
AIR FORCE MATERIEL COMMAND
HANSCOM AIR FORCE BASE, MA 01731-3010

"This technical report has been reviewed and is approved for publication."

(Signature)
CAPT MARK A. CLOUTIER
Contract Manager

(Signature)
DONALD E. BEDO
Chief
Measurements Branch

(Signature)
ROGER A. VAN TASSEL
Director
Optical Environment Division

This report has been reviewed by the ESC Public Affairs Office (PA) and is releasable to the National Technical Information Service (NTIS).

Qualified requestors may obtain additional copies from the Defense Technical Information Center (DTIC). All others should apply to the National Technical Information Service (NTIS).

If your address has changed, or if you wish to be removed from the mailing list, or if the addressee is no longer employed by your organization, please notify PL/TSI, 29 Randolph Rd. Hanscom AFB, MA 01731-3010. This will assist us in maintaining a current mailing list.

Do not return copies of this report unless contractual obligations or notices on a specific document requires that it be returned.

REPORT DOCUMENTATION PAGE

Form Approved
OMB No. 0704-0188

1. AGENCY USE ONLY *(Leave blank)*	2. REPORT DATE	3. REPORT TYPE AND DATES COVERED
	23 DEC 1993	Scientific Report No. 7

4. TITLE AND SUBTITLE

A Study of the Impact of Cirrus Clouds on High Altitude, Long Horizontal Path Laser Transmission.

5. FUNDING NUMBERS

PR 35160 F
PR 7670 TA 15 WUBB
Contract F19628-91-C-0093

6. AUTHOR(S)

G.G. Koenig, D.R. Longtin, J.R. Hummel

7. PERFORMING ORGANIZATION NAME(S) AND ADDRESS(ES)

SPARTA, Inc.
24 Hartwell Avenue
Lexington, MA 02173

8. PERFORMING ORGANIZATION REPORT NUMBER

LTR93-016

9. SPONSORING / MONITORING AGENCY NAME(S) AND ADDRESS(ES)

Phillips Laboratory
29 Randolph Road
Hanscom AFB, MA 01731-3010

Contract Manager: Capt. Mark Cloutier/GPOA

10. SPONSORING / MONITORING AGENCY REPORT NUMBER

PL-TR-93-2263

11. SUPPLEMENTARY NOTES

12a. DISTRIBUTION / AVAILABILITY STATEMENT

Approved For Public Release; Distribution Unlimited

12b. DISTRIBUTION CODE

13. ABSTRACT *(Maximum 200 words)*

The Geophysics Directorate of the USAF Phillips Laboratory is supporting efforts to estimate the environmental impacts on the proposed Airborne Laser (ABL) system, a laser system being considered for theater missile defense. One of the environmental factors of particular concern is cirrus clouds which can be found at the proposed levels for the ABL system.

Cirrus clouds can have spatial extents ranging from several tens of meters to several thousands of kilometers and are found at altitudes ranging from 4.0 to 20.0 kilometers. They are very persistent, and have a wide range of optical properties. Even cirrus clouds that have very low extinction coefficients, thus rendering them not visible for most viewing geometries, can have an effect on an Electro-Optic (EO) system if the cirrus optical path of the EO system is fairly long. Cirrus clouds with low extinction coefficients are difficullt to remotely sense with either ground or space based systems. Therefore, many of the present cirrus cloud databases contain incomplete information about optically thin cirrus clouds. The problem of determining cirrus cloud physical and optical properties is compounded by the high altitude location of these clouds. Recently, a number of programs have been conducted to investigate the physical and optical properties of cirrus clouds because of their unique impact on the global climate. These databases provide information that can be applied to studies of the impacts of cirrus on EO systems operating at cirrus cloud altitude and above. The purpose of this report is to provide general background information about cirrus clouds, some of the available cirrus cloud databases, and estimates of the impact of cirrus clouds on the proposed ABL system.

14. SUBJECT TERMS

ABL, Laser, Troposphere, Stratosphere, Transmission, Extinction, Optical Depth, Subvisual Cirrus, Thin Cirrus, Opaque Cirrus, Microphysical

15. NUMBER OF PAGES

38

16. PRICE CODE

17. SECURITY CLASSIFICATION OF REPORT	18. SECURITY CLASSIFICATION OF THIS PAGE	19. SECURITY CLASSIFICATION OF ABSTRACT	20. LIMITATION OF ABSTRACT
UNCLASSIFIED	UNCLASSIFIED	UNCLASSIFIED	SAR

Contents

Figures

Tables

A STUDY OF THE IMPACT OF CIRRUS CLOUDS ON HIGH ALTITUDE, LONG HORIZONTAL PATH LASER TRANSMISSION

1. INTRODUCTION

1.1 Background and Purpose of this Study

There is no doubt that clouds can have an impact on air operations. Historically, the primary concern has been to understand the impact of clouds on flying safety and satellite reconnaissance. In recent years, however, the focus has also included the impact of clouds on electro-optical sensors and proposed high energy lasers systems for strategic and theater missile defense. The impact of clouds on these systems is dependent on the spatial and temporal cloud distributions, and the optical and microphysical properties of the clouds. Liou *et al.*[1] has developed a model for InfRared (IR) transmission through thin and subvisual cirrus for passive IR target detection that not only takes into consideration the influence of cirrus in the foreground on target detection, but also the impact of cirrus in the background.

The Geophysics Directorate of the USAF Phillips Laboratory is supporting efforts to estimate the environmental impacts on the proposed AirBorne Laser (ABL) system, a laser system being considered for theater missile defense. One of the environmental factors of particular concern is cirrus clouds which can be found at the proposed flight levels for the ABL system. Although most cirrus clouds are generally thin when viewed vertically, they can have considerable horizontal extents and degrade the transmission for a laser system that propagates along a predominantly horizontal path, such as the ABL system.

---

[1] Liou K. N., Takano,Y., Ou, S.C., A. Heymsfield, and W. Kreiss (1990) Infrared transmission through cirrus clouds: A radiative model for target detection, *Appl. Optics*, **29**, 1886-1896.

The purpose of this study is to investigate the impact of cirrus clouds on the proposed ABL system. The study was conducted in two parts. The first part surveyed the available data bases on cirrus phenomenology and summarized the results. The second part of the study estimated the impacts of cirrus clouds on the transmission of the ABL system for the proposed threat scenarios.

1.2 Organization of the Report

Section 2 of the report presents an overview of cirrus cloud phenomenology. Section 3 presents cirrus-related results from two field programs co-sponsored by the Geophysics Directorate, the South Atlantic Backscatter Lidar Experiment[2] (SABLE) and the Global Atlantic Backscatter Lidar Experiment (GABLE). Section 4 looks at the impact of cirrus on long path laser transmission using proposed ABL engagement scenarios and Section 5 presents a summary and recommendations for additional studies.

[2] Alejandro, S.B., Koenig, G.G., Vaughan, J.M. and Davies, P.H. (1990) SABLE: A South Atlantic aerosol backscatter measurement program, *Bull. Amer. Meteor. Soc.*, 71:281-287.

2. CIRRUS CLOUD OVERVIEW

2.1 General Characteristics of Cirrus Clouds

Cirrus clouds are unique in that they are composed of ice crystals, mainly complex non spherical columns, plates, and bullet rosettes.[3] Cirrus clouds are global in nature with horizontal extents ranging from several tens of meters to several thousands of kilometers. They are also relatively stable and persistent, occurring mainly in the upper troposphere and lower stratosphere. From a radiative standpoint they tend to be semitransparent and non black (emissivities of less than one). (The reader is referred to Liou[4] for a thorough review of cirrus cloud composition, structure, and radiative properties).

Owing to their semitransparent and non black nature, cirrus clouds have been grouped into three general categories based on their optical characteristics: subvisual (or subvisible), thin, and opaque cirrus. Thin cirrus clouds are bluish in appearance and are semitransparent and non black, while subvisual cirrus are also semitransparent and non-black but can only be observed under certain viewing conditions.

Subvisual cirrus can be seen when the optical depth, the product of the extinction coefficient times the cloud path length, becomes large due to the long path length through the cirrus layer. For a ground observer these conditions can occur for low sun elevation angles (sunset and sunrise) and hence the term sunset or sunrise cirrus is sometimes used. For an observer in an aircraft, these conditions occur when the aircraft is above the cirrus layer and the observer is looking in a nearly horizontal direction. If subvisual cirrus is present under these viewing conditions, the aircraft observer may report a thin gray or dark band on the horizon depending on the natural illumination of the subvisual cirrus cloud layer.

Detection of subvisual cirrus is usually accomplished with lidar systems. Using a lidar system operating at 0.694 μm, Sassen *et al.*[5] have classified the three categories of cirrus based on the inverted cloud optical depth (τ_c). Subvisual to barely visual cirrus have optical depths $\tau_c \leq 0.03$, thin cirrus optical depths are in the range from $0.03 \leq \tau_c \leq 0.3$, and opaque cirrus have optical depths > 0.3.

2.2 Recent Measurement Programs

Cirrus clouds are of extreme importance on the earth-atmosphere energy balance. Unfortunately, there is an incomplete knowledge of the spatial and temporal distribution of cirrus clouds, and only a very superficial knowledge of the optical and microphysical properties of cirrus clouds. This has inspired a number of major international research programs to correct some of these deficiencies. Some of these programs are:

---

[3] Heymsfield A. J. and C. M. R. Platt, C.M.R. (1984) A parameterization of particle size spectrum of ice clouds in terms of the ambient temperature and the ice water content, *J. Atmos Sci*, **41**:846-855.

[4] Liou, K.N., (1986) Influence of cirrus clouds on weather and climate processes: A global perspective, *Mon. Wea. Rev.*, **114**:1167-1197.

[5] Sassen K. and Cho, B.S. (1992) Subvisual-Thin Cirrus Lidar Dataset for Satellite Verification and Climatological Research, *J. Appl. Meteor.*, **31**:1275-1285.

- The International Satellite Cloud Climatology Program[6] (ISCCP), a ten year program initiated in 1983 with the objective of developing an extensive satellite cloud database
- The First ISCCP Regional Experiment[7] (FIRE) which has the objective of understanding the mechanisms of cirrus and marine stratocumulus formation and the investigation of cirrus and marine stratocumulus optical and microphysical properties
- The European International Cirrus Experiment (ICE) with the objective of understanding the mechanisms of cirrus formation and the investigation of cirrus optical and microphysical properties
- The Experimental Cloud Lidar Pilot Study[8] (ECLIPS) program which has the objectives of obtaining a long-term cloud base height and cloud optical properties database, improving satellite cloud retrieval algorithms by using coincident lidar data, and improving satellite based predictions of the surface energy balance
- Cirrus Remote Sensing Pilot Experiment[9] (CRSPE) program with objectives of characterizing the horizontal and vertical cirrus cloud inhomogeneities, parameterization of visible and infrared cirrus optical properties, verification of satellite cloud retrieval methods, statistical description of cirrus spatial scales, and a database for comparison with radiative transfer models.

2.3 Existing Cloud Databases

A number of programs have specifically targeted the development of regional or global cloud databases. These databases have been generated using different techniques to determine cirrus physical, and in some cases, optical properties.

2.3.1 Lidar Measurements

Lidars are one of the most accurate tools for determining cirrus cloud base height, and depending on the optical thickness of the cirrus cloud, the cloud top height. In addition, some ice particle morphology and optical properties can be obtained from lidar measurements (for example, from depolarization measurements and from lidar/radiometer coincident measurements). One of the major limitations of lidar measurements is that lidars provide only point measurements and are usually not operated continuously for any

---

[6] Schiffer R.A. and Rossow, W.B.(1983) The International Satellite Cloud Climatology Project (ISCCP): The first project of the world climate research programme, *Bull. Amer. Meteor. Soc.*, 64:2682-2694.

[7] Cox, S.K., McDougal, D.S., Randall, D.A., and Schiffer, R.A. (1987) FIRE-The First ISCCP Regional Experiment, *Bull. Amer. Meteor. Soc.*, 68:114-118.

[8] WCRP-14 (1988) "An Experimental Cloud Lidar Pilot Study (ECLIPS), report of the WCRP/CSIRO workshop on cloud base measurement, CSIRO, Mordialloc, Victoria, Australia, 29 February - 3 March 1988, WMO/TD-No. 251.

[9] Ackerman, S.A., Eloranta, E.W., Grund, C.J., Knuteson, R.O., Revercomb, H.E., Smith,W.L., and Wylie, D.P. (1993) University of Wisconsin cirrus remote sensing pilot experiment, *Bull. Amer Meteor. Soc.*, 74:1041-1049.

long period of time. Sassen *et al.*[5] have developed a lidar data set, for the ECLIPS program, based on lidar observations collected since December 1986 from the Facility for Atmospheric Remote Sensing (FARS) located at the University of Utah (40°46'00"N, 111°49'38"W). This data set consists of: cloud base, top, and effective mid cloud altitudes; the scattering ratio (the ratio of the lidar backscatter to the clear air lidar backscatter); physical and optical cloud thickness; and the depolarization ratio. The ECLIPS data set offers the potential of obtaining cirrus cloud information based on lidar measurements and coincident satellite information at a number of locations world wide.

2.3.2 Balloon-Borne Measurements

Data collected using balloon-borne instruments is a potential source of high quality cirrus cloud information. One such source is the balloon borne frost-point hygrometers launched monthly from several locations by NOAA. The balloons were launched on days with little or no opaque clouds in the sky and provide vertical profiles of tropospheric and stratospheric water-vapor concentration based on the dry-bulb and frost-point temperature measurements. Forty-four percent of the frost-point hygrometer measurements from 1981 to 1988 over Boulder, Colorado, indicate the presence of at least one saturated layer at cirrus cloud altitudes (Oltmans[10]). During FIRE II, which was conducted at Coffeeville, Kansas, a Formvar replicator was flown from a balloon platform and very high quality ice crystal images were obtained. Due to the slow ascent rate of the balloon very few of the crystals were damaged upon impact with the replicating surface.

2.3.3 Surface Observations

Surface observations are still a valuable source of cloud information. London[11] and Hahn *et al* [12] have developed cloud climatologies based on surface observations. The Air Force's 3DNEPH[13] cloud analysis (now known as the RTNEPH) has been archived since the earlier 1970's. The 3DNEPH is a cloud database based on both surface observations and the analysis of Defense Meteorological Satellite Program (DMSP) satellite imagery using a threshold technique. However, cloud databases based on surface observation provide only limited spatial coverage and tend to underestimate cirrus cloud amounts because optically thin cirrus clouds can only be observed under certain viewing conditions or they may be obscured by lower cloud layers.

---

[10] Oltmans, S.J., (1986) "Water vapor profiles for Washington, DC; Boulder, CO; Palestine, TX; Laramie, WY; and Fairbanks, AK; during the period 1947 to 1985", NOAA Data Rep. ERL-ARL-7.

[11] London, J., (1957) "A study of the atmospheric heat balance. Final Rep.,": Contract AF19(122)-165, Dept. of Meteor. and Oceanogr., New York University, 99 pp. (ASTIA 117 227 Air Force Geophysics Laboratory, Hanscom AFB, MA. 01730.)

[12] Hahn, C.J., Warren, S.G., London, J., Chervin R.M., and Jenne, R. (1982) *Atlas of Simultaneous Occurrence of Different Cloud Types over the Ocean.* NCAR/TN-201+STR, National Center for Atmospheric Research, 212 pp.

[13] Fye, F.K., (1978) "The AFGWC automated cloud analysis model," *Tech. Memo. 78-002*, Air Force Global Weather Central, Offut Air Force Base, NE, 97 pp.

2.3.4 Satellite Measurements

One of the major sources of cloud information is from satellite data. Statistical, threshold, and radiative transport techniques are used to analyze the satellite information to obtain cloud cover, cloud type, cloud height information. Because of the unique radiative properties of cirrus clouds and their impact on climate, most cloud databases provide information on the spatial and temporal distribution of high clouds and in some cases information on the optical properties of these clouds. The cloud databases derived from single channel infrared radiance in the 10-12μm window region from polar orbiting satellites provide good aerial coverage but have limited vertical and temporal resolution. The temporal resolution can be enhanced by utilizing information from Geostationary Operational Environmental Satellite(s). However, as pointed out by Liou[4], some thin cirrus, and thus most subvisual cirrus, may be undetected by satellite visible and infrared channels. In the case of semitransparent cirrus clouds, the cloud height determination may be in error due to contamination of the cloud infrared radiance values by the transmission of infrared radiance from below the cloud.

Initial results from ISSCP on the development of a global cloud climatology have been reported by Rossow *et al.*[14] and a compendium of the available data products can be found in Rossow *et al.*[15] Stowe *et al.*[16] have developed a global cloud climatology based on Nimbus-7 data while Barton[17] has developed an upper level cloud climatology from satellite data.

Multispectral observations from the VAS [Visible-Infrared Spin Scan Radiometer (VISSR) Atmospheric Sounder] geostationary satellite data in the carbon dioxide 15 μm absorption band have been analyzed by Menzel *et al*[18], using CO_2 "slicing" algorithms, to obtain cirrus cloud cover statistics, cloud top pressure, and cloud emissivity for the continental United States. This four year climatology indicates cirrus clouds are found in 25 to 30 % of the observations and exhibit very little seasonal change. It is estimated that due to the limited sensitivity, approximately 5% of the thin cirrus is missed. Using this method, cloud tops are determined radiatively and are near the physical cloud top for optically thick clouds and near the cloud middle for optically thin clouds. The corresponding cloud top pressure may be off as much as 100 mbs when thin cirrus overlie an optically thick middle cloud layer. In a comparison of VAS cloud top data with lidar data, Grund *et al.*[19] found the CO_2 "slicing" method underestimated the cloud top pressure by approximately 65 mbs (1.0 to 1.5 km). The typical corrected VAS cirrus cloud top altitudes were in the 9 to 10 km range with some values as high as 13 km.

---

[14] Rossow, W.B., and Lucis, A.A. (1990) Global seasonal cloud variations from satellite radiance measurements part II: Cloud properrties and radiative effects, *J. Climate*, 3:1204-1253.

[15] Rossow, W.B., and Schiffer, R.A. (1991) International satellite cloud climate project products, *Bull. Amer. Meteor. Soc.*, 72: 2-21.

[16] Stowe, L.L., Yeh, H.Y.M, Eck, T.F., Wellemeyer, G.G., Kyle, H.L,. and the NIMBUS-7 cloud data processing team (1989) Nimbus-7 global cloud climatology part II: First year results, *J Climate*, 2:671-709.

[17] Barton, I.J. (1983) Upper level cloud climatology from an orbiting satellite, *J. Atmos. Sci.*, 40:435-447.

[18] Menzel, W.P., Wylie, D.P., and Strabala, K.I. (1992) Seasonal and diurnal changes in cirrus clouds as seen in four years observations with the VAS, *J. Appl. Meteor.*, 31:370-384.

[19] Grund, C.J., and Wylie, D. (1989) Lidar validations of VAS; cirrus cloud height determinations. AIAA paper 89-0804, 27th Aerospace Sciences Meeting, January 9-21, Reno, Nevada.

Barton[17] developed an upper level zonal average cloud amount and height data base from two narrow-band channels in the H_2O-CO_2 2.7 μm band on the Nimbus 5 satellite. Due to the strong absorption in this region, only reflected energy from clouds higher than approximately 6 km is detected by the radiometer. The maximum zonal average upper level cloud cover in the mid latitudes is on the order of 25% while the maximum in the equatorial region is on the order of 30%. There are relatively cloud free regions around 80° N and S (where cloud cover is generally only several percent) and at 25° N and 20° S (where the cloud cover is on the order of 15%). The position of the upper level cloud zonal average minimum and maximum cloud cover exhibit seasonal variations on the order of 10° latitude.

Zonal and geographical distributions of cirrus clouds have been developed by Woodbury *et al.*[20] from data obtained with the Stratospheric Aerosol and Gas Experiment (SAGE) satellite. The SAGE data have been analyzed to produce profiles of 1.0 μm extinction in the range from 1.0×10^{-2} to 2.0×10^{-5} km^{-1} with a vertical resolution of 1 km. The data were analyzed in the altitude range from 1 km above the tropopause to a height equivalent to 70% of the tropopause height or 8 km, depending on which was greater. Extinction coefficient values greater than 8.0×10^{-3} km^{-1} were considered to be associated with optically thick cirrus clouds, while extinction coefficients in the range from 8.0×10^{-4} to 8.0×10^{-3} km^{-1} were considered to be associated with optically thin cirrus. The mean cirrus cloud heights as determined from 11 months of SAGE observations, range from 7.0 km at 65° N and S to 13.5 km at 5° S. Since SAGE observations at the lower altitudes are less frequent than at the higher altitudes there is reason to believe the mean altitudes from the SAGE data are biased toward the higher altitudes.

While the SAGE data provide excellent vertical profile information with fairly high sensitivity, it does not provide good aerial coverage. In addition, the cirrus distributions are reported as frequencies of occurrence of extinction coefficient values, since it is not possible to determine the cloud coverage. This is a consequence of the effective field-of-view (FOV) of the satellite (0.5 km x 200 km). For a single observation with an extinction coefficient value that is greater than the cloud threshold value, it is not possible to tell whether a single cloud occurs in the FOV or if there are multiple clouds. In addition, two consecutive profiles that have high extinction coefficients values may be a manifestation of the same cloud or different localized clouds. Finally, based on the observed 0.694 μm lidar optical depth, cloud base, and cloud top information in Table 1 from Sassen *et al.*[5], the average extinction coefficient for subvisual cirrus is 0.017 km^{-1} with a range of 0.007 to 0.035 km^{-1}. The corresponding values for thin cirrus are 0.049 km^{-1} and 0.012 to 0.169 km^{-1}, respectively. The extinction difference due to the wavelength difference between the lidar (0.694 μm) and the satellite observations (1.0 μm) should only be on the order of a few percent for cirrus clouds. This implies the range of extinction values associated with the SAGE analysis are more characteristic of subvisual cirrus.

---

[20] Woodbury, G.E., and McCormick, M.P. (1986) Zonal and geographical distributions of cirrus clouds determined from SAGE data, *J. Geophy. Res.*, 91:2775-2785.

2.4 Cirrus Cloud Dynamics

As indicated above, the horizontal extent of cirrus clouds is from several tens of meters to several thousands of kilometers depending on the cloud formation dynamics. These dynamic features can be synoptic and mesoscale disturbances or single convective cells. In general, there are four major mechanisms that can result in the generation of cirrus clouds: wind shears, convective activity, synoptic systems, and the formation of cirrus due to man's activity. The last mechanism is associated with the formation of contrails associated with high flying jet aircraft. It is believed that the frequency of occurrence of contrails is great enough, especially along the major air routes, to have an impact on surface temperature trends. Both Liou *et al.*[21] and Changon[22] investigated the effects of contrail cirrus on the surface temperature trends.

Cirrus shields are usually associated with trough/ridge systems and frontal systems. Figure 1 shows an image taken from the Geostationary Orbiting Environmental Satellite of a frontal system extending from a low pressure system located to the NNW of the Great Lakes along the eastern seaboard of the United States down to the lower left hand corner of the image. There is a cirrus shield associated with a weather system forming along the frontal boundary as indicated by the arrow. In addition, there are a number of convective clusters along the frontal system in the lower left hand corner of the image. South of the frontal zone there appears to be several cirrus shields, most likely associated with either convective activity or upper level disturbances. From this particular image, it is not possible to determine the extent of the cirrus shields, but as indicated, there are several dynamic features that appear to be responsible for the cirrus evident in the satellite image.

Another potential source of cirrus is from regions of wind shear, especially regions associated with mid-latitude, polar and sub-tropical jet streams. Using time lapse photography, Conover[23] did an extensive study of cirrus clouds associated with jet streams. He found that cirrus clouds are located to the southwest of the jet stream and were usually 45 to 65 km wide and several hundred kilometers long. Based on the visual appearance of the cirrus clouds, he categorized the cirrus as either sheets, streaks, bands, or random (cells). The observed jet stream cirrus was usually parallel to regions of high level temperature discontinuities and in regions of strong vertical shear. Cirrus sheets formed in regions of more stable lapse rates, while the random, or cell, cirrus formed in regions of conditional unstable lapse rates (the lapse rate is between the pseudo adiabatic and dry adiabatic lapse rate). Conover indicates that random cirrus may form in the region between adjacent horizontal Bernard cells. He found cirrus cell spacing ranged from 0.2 to 2.3 km with an average cell size of 1.2 km and the vortices or Bernard cells ranged in size from 0.1 to 25 km with an average size of 2.2 km.

---

[21] Liou, K.N., Ou, S.C. and Koenig, G.G. (1990) "An investigation on the climate effect of contrail cirrus", Lecture Notes in Engineering Air Traffic & Environment: Background Tendency and Potential Global Atmospheric Effects, Ed U. Schumann, Springer-Verlag.

[22] Changnon, S. A. Jr., (1981) Midwestern cloud, sunshine, and temperature trends since 1961: Possible evidence of jet contrail effects, *J. Appl. Meteor.*, **20**:496-508.

[23] Conover, J., (1960) Cirrus patterns and related air motions near the jet stream as derived by photography, *J. Meteor.*, **17**:532-546.

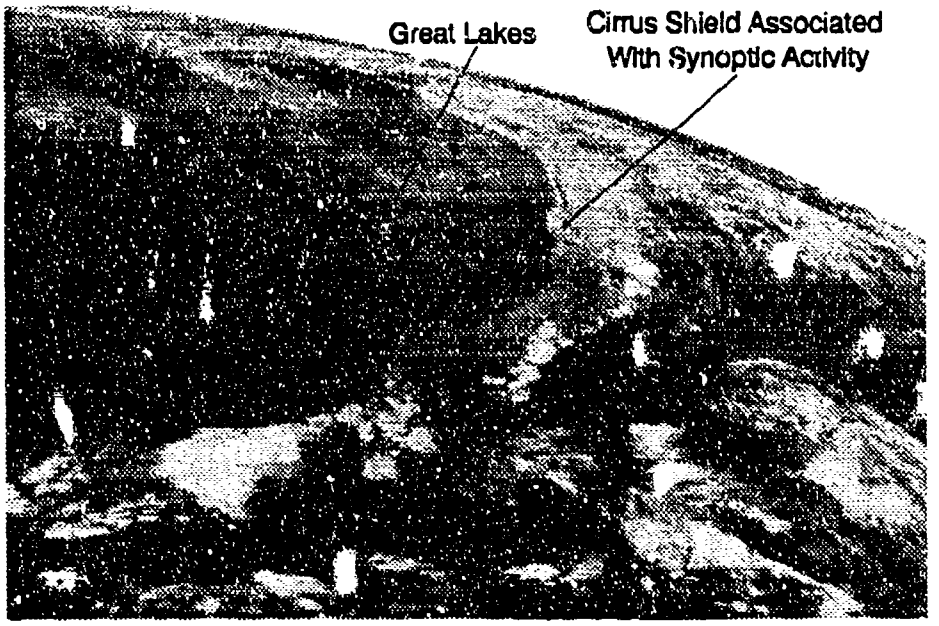

Figure 1. An Example of an Infrared Satellite Image Containing Cirrus Clouds Associated with a Frontal System. A (faint) cirrus shield is found to the west of the main body of clouds

In a series of articles Heymsfield,[24,25,26] investigated the formation and longevity of cirrus uncinus clouds (comma shaped cirrus clouds). He speculated on two potential mechanisms for the formation of the cirrus uncinus clouds: one method involved convective cell generation associated with the lifting of a layer, while the second method involved a stable layer just below the cirrus uncinus head with convection associated with either gravity, critical, or Kelvin-Helmholtz waves. He attributed the longevity of the cirrus to evaporative cooling (evaporation of ice crystals in the trail of the cloud) and convergence/divergence associated with wind shears. More recently Starr and Cox[27] have developed a high resolution (1 km) two dimensional model to investigate the role of various physical processes involved in the formation and maintenance of cirriform clouds.

---

[24] Heymsfield, A.J., (1975) Cirrus uncinus generating cells and the evolution of cirriform clouds. Part I: Aircraft observations of the growth of the ice phase, *J. Atmos. Sci.*, 32,:799-808.

[25] Heymsfield, A.J., (1975) Cirrus uncinus generating cells and the evolution of cirriform clouds. Part II: The structure and circulations of the cirrus uncinus generating head, *J. Atmos. Sci.*, 32:809-819.

[26] Heymsfield, A.J., (1975) Cirrus uncinus generating cells and the evolution of cirriform clouds. Part III: Numerical computations of the growth of the ice phase, *J Atmos. Sci.*, 32:820-830.

[27] Starr, D.O., and Cox, S.K. (1985) Cirrus clouds. Part II: Numerical experiments on the formation and maintenance of cirrus, *J. Atmos. Sci.*, 42:2682-2694.

2.5 Cirrus Cloud Altitudes

Cirrus clouds exhibit considerable spatial and temporal variability. Figure 2 is an image generated from the backscatter information obtained with the University of Wisconsin Volume Imaging Lidar (VIL). The spatial variability of the lidar backscatter associated with cirrus is very evident in this image. Time series of VIL imagery clearly show the temporal variability of cirrus clouds.

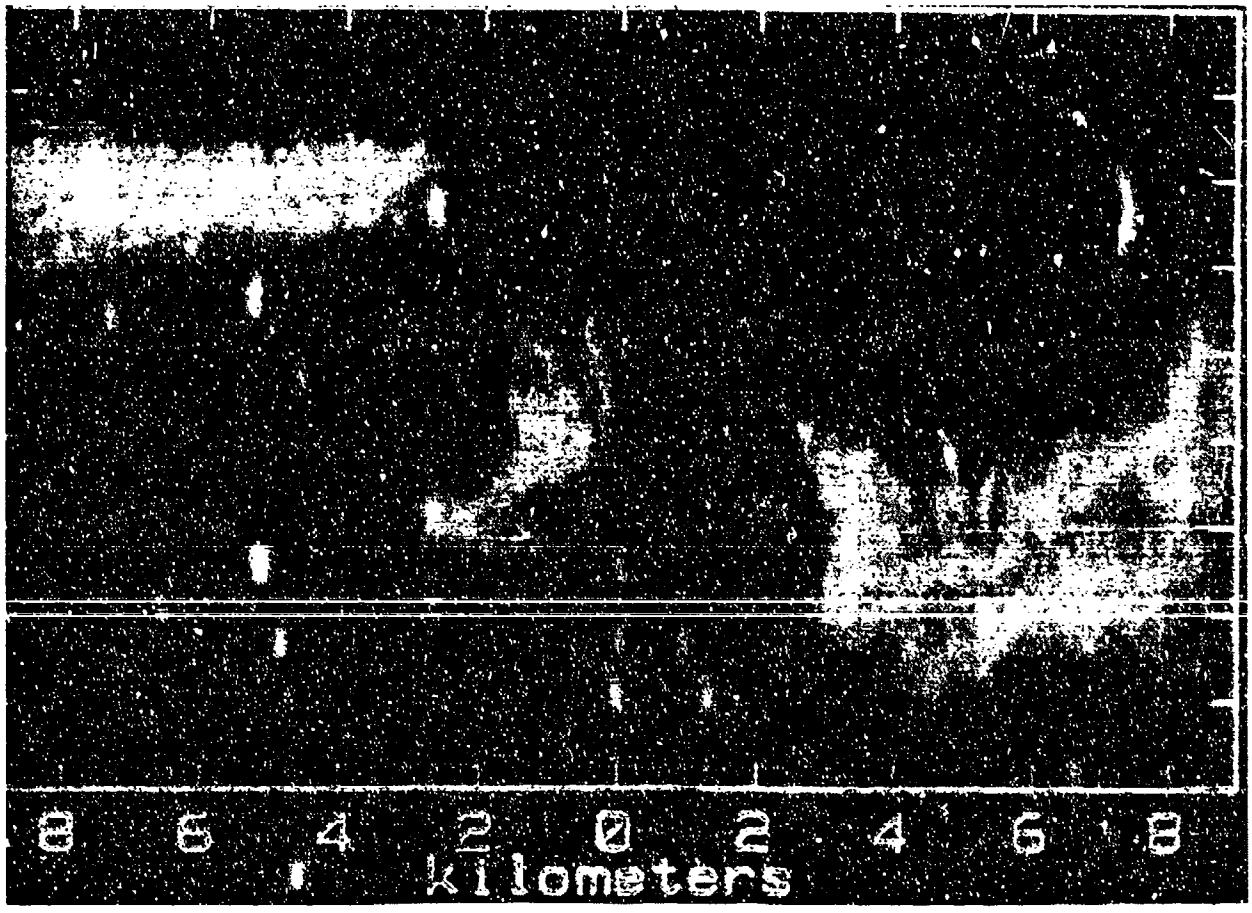

Figure 2. Example of an Image of a Cirrus Cloud Obtained by the University of Wisconsin Volume Imaging Lidar System. The Vertical Scale Extends From 9.8 to 11.6 km

Uthe, in support of the InfRared Search and Track (IRST) program, made airborne lidar and radiometric measurements to characterize high altitude clouds. From a series of airborne lidar measurements in the vicinity of Kwajalen Island, he detected subvisual cirrus in the altitude range from 40,000 to 60,000 ft (12.2 to 18.3 km). In measurements made over the Gulf of Mexico he detected cirrus cloud bases in the altitude range 35,000 to 50,000 ft (10.7 to 15.2 km). During one measurement episode, the lidar detected subvisual cirrus with a cloud base at 40,000 ft (12.2 km) and a cloud top at 50,000 ft (15.2 km). Heymsfield (unpublished) from an aircraft data set over the United States and the Marshall Islands, found optically thin cirrus clouds, that appeared as a haze, within two kilometers of the tropopause on almost every flight.

Table 1 displays mid-cloud altitudes for different seasons generated from information given by Platt *et al.*[28] In addition to the mid cloud altitudes, Platt *et al*[28] also specified the cloud thickness. For summer the range was from 0.90 to 4.03 km, for winter it was 1.00 to 4.04 km, and for the tropics it was 0.82 to 3.20 km. Sassen[5] has also presented lidar derived cloud height information for subvisual and thin cirrus. This information has been summarized and reproduced in Figure 3.

Table 1. Mid Cloud Altitudes for Different Seasons and Locations Reported by Platt *et al.*[28]

Summer		Winter		Tropical	
Mid Cloud Altitude (km)	Number of Observations	Mid Cloud Altitude (km)	Number of Observations	Mid Cloud Altitude (km)	Number of Observations
-	-	-	-	15.34	337
11.77	140	-	-	13.78	576
11.33	417	11.30	1048	12.67	410
9.92	709	9.55	941	11.56	177
8.73	453	8.05	1026	-	-
7.88	495	6.76	621	-	-
6.52	368	5.60	112	-	-
5.52	9	-	-	-	-

Dowling *et al.*[27] recently summarized the physical properties of cirrus clouds and that information is given in Table 2. Dowling *et al.* indicate that the fractional cloud cover may be too low since the sensing systems and algorithms used to generate cloud databases frequently miss subvisual and thin cirrus clouds.

2.6 Cirrus Cloud Particle Sizes

It is interesting to note that the cloud ice crystal sizes ranged from 1 to 8,000 μm. Most of the instruments used to make *in situ* measurements of ice crystal sizes have minimum detection thresholds on the order of 25 μm. The existence of a small particle mode has been deduced from a comparison of theoretical cirrus cloud radiometric calculations and the observed radiometric values (Minnis *et al.*[29], Spinhirne and Hart,[30] and Wielicki *et*

[28] Platt, C.M.R., Scott, J.C., and Dilley, A.C. (1987) Remote sounding of high clouds. Part VI: Optical properties of midlatitude and tropical cirrus, *J. Atmos. Sci.*, 44:729-747.

[29] Minnis, P., Young, D.F., Sassen, K., Alvarez, J.M. and Grund, C.J. (1990) The 27-28 October 1986 FIRE IFO cirrus case study: Cirrus parameter relationships derived from satellite and lidar data, *Mon. Wea. Rev.*, 118:2426-2446.

[30] Spinhirne, J.D. and Hart, W.D. (1990) Cirrus structure and radiative parameters from airborne lidar and spectral radiometer observations: The 28 October 1986 FIRE study, *Mon. Wea. Rev.*, 118:2329-2343.

al.[31]) Sassen *et al.*[32] have suggested that the difference between the calculated radiative values and the measured radiative values for cirrus may be due to the complex nature of the ice crystals and not the presence of a small particle mode. If there is a small particle anomaly, it will impact the forward scattered laser radiation, especially if the Mie size parameter, the ratio of the particle circumference to the wavelength, is less than 25. For large size parameters, there is a strong forward scattering peak, while for smaller size parameters there is an increase in the scatter away from the forward direction (*e.g.* Muinonen.[33]). In addition, there is some evidence that many of the ice crystals may be hollow. Radiative transfer models currently do not model hollow ice crystals.

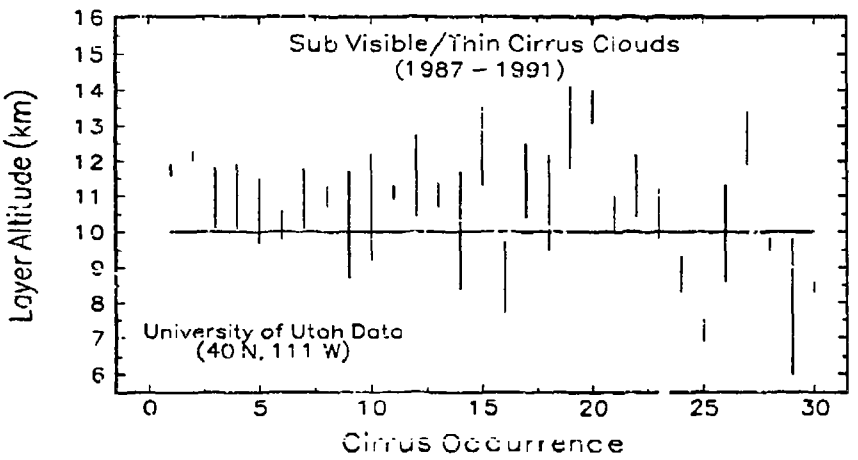

Figure 3. A Summary of Lidar-Derived Cloud Height Data for Sub Visible and Thin Cirrus Obtained From the Lidar System Operated at the University of Utah[5]

Table 2. A Summary of Physical Properties of Cirrus Clouds From the Work of Dowling *et al.*[22]

Property	Typical Value	Range
Cloud Thickness	1.5 km	0.1 - 8.0 km
Cloud Center Altitude	9.0 km	4.0 - 20.0 km
Ice Crystal Length	250 μm	1 - 8,000 μm
Fractional coverage	-	0.30 - 0.50

[31] Wielicki, B.A., Suttles, J.T., Heymsfield, A.J., Welch, R.W., Spinhirne, J.D., Wu, M.L.C., Starr, D.O., Parker, L,. and Ardnini, R.F. (1990) The 27-28 October 1986 FIRE IFO cirrus case study: Comparison of radiative transfer theory with observations by satellite and aircraft, *Mon. Wea. Rev.*, 118:2356-2376.

[32] Sassen, K., Heymsfield, A.J., and Starr, D.O. (1991) "Is there a cirrus small particle radiative anomaly?" preprint 7th conference on Atmospheric Radiation, July 23-27 1990, San Francisco, CA. J91-J95.

[33] Muinonen, K., (1989) Scattering of light by crystals: a modified Kirchoff approximation, *Appl. Opt.*, 28: 3044-3049.

3. SABLE/GABLE CIRRUS DATABASE

3.1 Program Overview

The basic objective of the SABLE and GABLE programs was to establish an aerosol lidar backscatter database in the vicinity of remote island locations in the north and south Atlantic. The SABLE programs were conducted from Ascension Island from 27 October to 9 November 1988 and 22 June to 16 July 1989, while the GABLE programs were conducted from Iceland from 15 to 18 May 1990 and the Azores from 9 to 22 August 1990. A ground-based lidar system and an aircraft-based Doppler laser system were used to collect aerosol backscatter information. Only backscatter information from the aircraft CO_2 (10.6 μm) laser is used in the analysis reported here. Information on the laser system can be found in Woodfield and Vaughn.[34] The laser system detects backscatter from a pencil-like volume approximately 150 meters in length and approximately 100 meters directly ahead of the aircraft. The system is calibrated and has a minimum backscatter coefficient, $\beta(\pi)$, detection capability of 3×10^{-12} m^{-1} sr^{-1}. The laser system was mounted in the bomb bay of a Canberra (B-57) aircraft. The Canberra has a maximum ceiling of approximately 53,000 feet (16.2 km).

3.2 Establishment of Cirrus Threshold

The first step in analyzing the SABLE/GABLE data was to establish the criteria used to determine backscatter coefficient values that were significantly greater than the anticipated molecular and background aerosol backscatter values. In addition to establishing a backscatter coefficient threshold, a temperature threshold was also established since, by definition, cirrus clouds are composed of ice crystals. Based on Rogers,[35] the temperature threshold was established as -20° C. This temperature corresponds to an altitude of approximately 8 km for the SABLE missions. From a preliminary analysis of SABLE data, Koenig (private communication, 1992) established the backscatter threshold as

$$\beta_\pi(10.6\ \mu m) = 8 \times 10^{-10}\ m^{-1}\ sr^{-1} \quad @\ 8\ km$$

and

$$\beta_\pi(10.6\ \mu m) = 4 \times 10^{-10}\ m^{-1}\ sr^{-1} \quad @\ 15\ km.$$

A scattering ratio of 1.5 has been used extensively to differentiate between clear sky and cloud backscatter returns. Using the Air Force Geophysics Laboratory (AFGL) tropical atmosphere[36] with a background tropospheric aerosol this threshold corresponds to

---

[34] Woodfield, A.A. and Vaughn, J.M. (1983) Airspeed and wind shear measurements with an airborne CO_2 CW laser, *Int. J. Aviation Safety*, 2:207-224.

[35] Rogers, R.R (1979) Chapter 8 "Formation and Growth of Ice Crystals" in *A Short Course in Cloud Physics*. Second Edition, Pergamon Press International, New York, NY.

[36] Anderson, G.P., Clough, S.A., Kneizys, F.X., Chetwynd, J.H., and Shettle, E.P. (1986) "AFGL Atmospheric Constituent Profiles (0 - 120 km)", Air Force Geophysics Laboratory, Hanscom AFB, MA, AFGL-TR-86-0110, 15 May, ADA 175173.

$$\beta_\pi(10.6\ \mu m) = 4.2 \times 10^{-10}\ m^{-1}\ sr^{-1} \quad @\ 8\ km$$

and

$$\beta_\pi(10.6\ \mu m) = 1.0 \times 10^{-10}\ m^{-1}\ sr^{-1} \quad @\ 15\ km.$$

For the results to be presented, the backscatter threshold value for cirrus was taken as

$$\beta_\pi(10.6\ \mu m) = 8.5 \times 10^{-10}\ m^{-1}\ sr^{-1}$$

for all altitudes with temperatures below -20° C. The details on the procedures used to analyze the SABLE and GABLE data sets and the comprehensive statistics associated with the analysis are given in Longtin *et al.*[37]

3.3 Cirrus Analysis

Figure 4 represents the results of an analysis of the vertical thicknesses of the cirrus encountered during the SABLE 88, SABLE 89, and GABLE 90 field programs. As anticipated, the cirrus levels associated with the SABLE field program, which were conducted at approximately 8° S, are higher than the levels associated with the GABLE programs, which was conducted at approximately 64° and 39° N. These trends occur because cirrus is frequently found in the vicinity of the tropopause, which is higher in the tropics than at mid and high latitude locations.

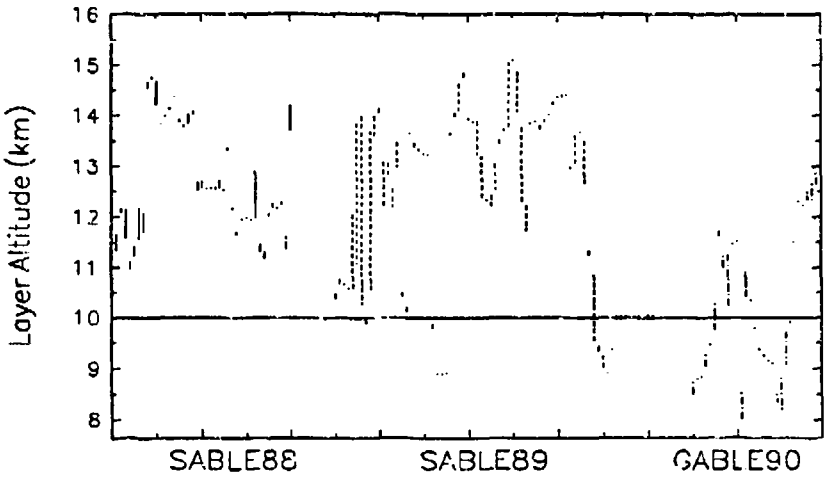

Figure 4. A Summary of the Cirrus Altitude Ranges Detected During the SABLE/GABLE Programs

A statistical analysis of the cirrus thicknesses was also made. Table 3 lists the number of occurrences, N and the percent occurrence, P(N), for a given cirrus vertical thickness measured during the SABLE/GABLE programs.

---

[37] Longtin, D.R., Koenig, G.G., Hummel, J.R., and Jones, J.R. (1993) "Analysis of Aircraft-Based Lidar Backscatter Measurements from the SABLE and GABLE Programs," Phillips Laboratory, Hanscom AFB, MA, PL-TR-93-2026.

Table 3. Number of Occurrence, N, and Percent Occurrence, P(N), of the Inferred Vertical Thicknesses of Cirrus Clouds Inferred From the SABLE/GABLE Field Programs

VERTICAL THICKNESS (km)	SABLE 88		SABLE 89		GABLE 90		TOTALS OVER SABLE/GABLE	
	N	P(N)	N	P(N)	N	P(N)	N	P(N)
0.000-0.050	19	47.5	32	44.4	12	40.0	63	44.4
0.051-0.099	04	10.0	13	8.1	3	10.0	20	14.1
0.100-0.199	08	20.0	5	6.9	4	13.3	17	12.0
0.200-0.399	04	10.0	4	5.6	5	16.7	13	9.2
0.400-0.599	03	7.5	6	8.3	3	10.0	12	8.4
0.600-0.799	01	2.5	1	1.4	2	6.7	4	2.8
0.800-0.999	01	2.5	4	5.6	0	0.0	5	3.5
1.000-1.999	00	0.0	4	5.6	1	3.3	5	3.5
> 2.000	00	0.0	3	4.2	0	0.0	3	2.1

Using the thresholds established to distinguish clear air backscatter returns from cirrus backscatter returns, the horizontal extent of the cirrus was determined from the elapsed time in a cirrus layer and the aircraft speed. It should be noted that these horizontal extents are not straight-line distances due to the nature of the flight tracks. The pseudo-horizontal extents from the SABLE/GABLE programs are given in Figure 5.

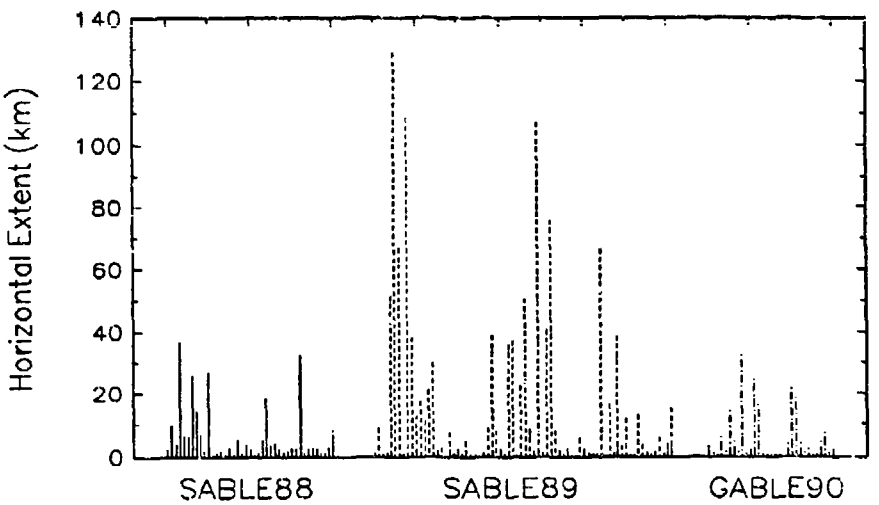

Figure 5. Cirrus Horizontal Extents as Determined From the SABLE and GABLE Backscatter Laser Data.

Figures 6 and 7 display 3-dimensional flight tracks and the extent of the cirrus for Flight 6 from SABLE 88 and Flight 31 from SABLE 89. For Flight 31, the cirrus extends over approximately four degrees of longitude and three degrees of latitude. On the outward leg of the flight track, the aircraft was in cirrus almost all the time from an altitude of 10.5 to 14.0 km, which corresponds to a horizontal extent of over 300 km.

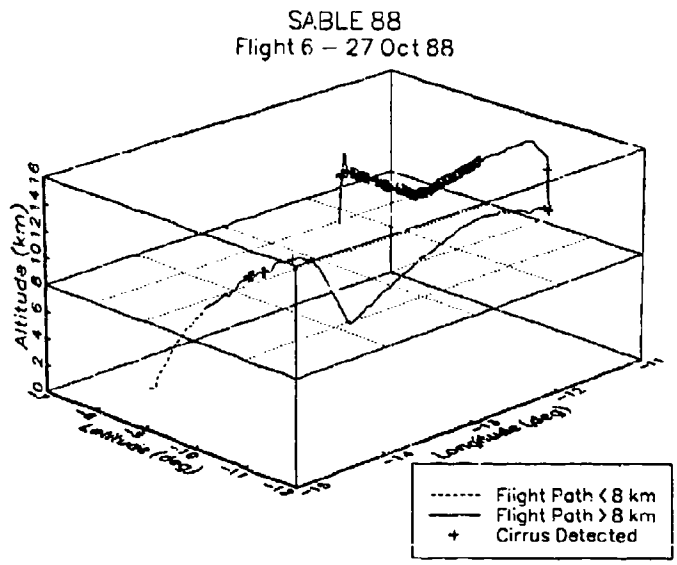

Figure 6. Flight Track Showing the Cirrus Detected During Flight 6 on 27 October 1988 From the SABLE88 Field Program

It is possible to convert the cirrus backscatter coefficients obtained using the indicated thresholds to a vertical optical depth (τ) and to categorize the cirrus based on the vertical optical depth (*e.g.* subvisual, thin, or opaque.) The vertical optical depth is defined as

$$\tau(0.55\mu m) = \frac{1}{k}\int_{z_{min}}^{z_{max}} \beta_{\pi}(10.6\mu m, z)\,dz$$

where k is the scaling factor used to relate the 10.6 μm backscatter coefficient to the 0.55 μm extinction coefficient. For this analysis, k was set equal to 2.2×10^{-4} sr^{-1}. When more than one backscatter coefficient value occurred at a given altitude, the values were averaged using a logarithmic average. Table 4 gives the results of this analysis, showing the number of cases and the frequency of occurrence for the three categories of cirrus based on the vertical optical depth.

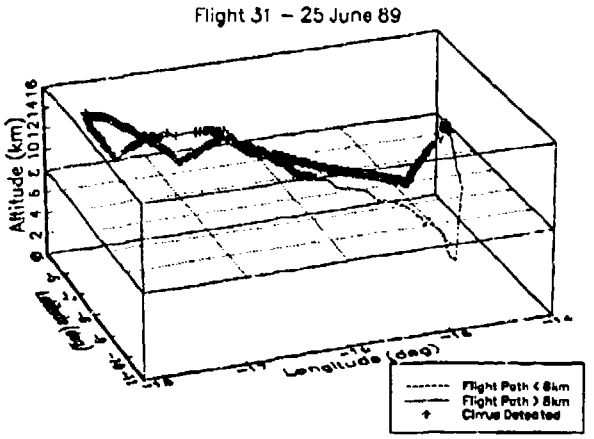

Partial Listing of Detected Cirrus Clouds

Altitude Range (km)	Distance in Cloud (km)
10.5 - 12.0	51.6
11.1 - 13.9	128.9
10.3 - 14.0	66.6
10.6 - 14.7	108.5
13.6 - 14.0	38.0

Figure 7. Flight Track Showing the Cirrus Detected During Flight 31 on 25 June 1989 From the SABLE89 Field Program and a Partial Listing of the Extent of the Cirrus

Table 4. Number of Cases and Frequency of Occurrence of Subvisual, Thin, and Thick Cirrus Classified on the Basis of Vertical Optical Depth

CIRRUS CATEGORY	VERTICAL OPTICAL DEPTH	SABLE 88 N	SABLE 88 P(N)	SABLE 89 N	SABLE 89 P(N)	GABLE 90 N	GABLE 90 P(N)
-	<0.001	22	55.0	40	55.6	16	53.3
Subvisual	0.001 - 0.003	14	35.0	12	16.7	9	30.0
Thin	0.030 - 0.300	2	5.0	7	9.7	4	13.3
Thick	>0.300	2	5.0	13	18.1	1	3.3

During SABLE88, 7.37 % of the backscatter returns above 8 km were greater than 6.0×10^{-10} m^{-1} sr^{-1}. Over 99% of the backscatter values that exceeded this threshold occurred at an altitude greater than 10 km. During SABLE89, approximately 50.0 % of the backscatter returns above 8 km were greater than 6.0×10^{-10} m^{-1} sr^{-1}. Over 90% of the backscatter values that exceeded this threshold occurred at an altitude greater than 10 km, and 68% of the returns that were classified as cirrus were in the altitude range from 10 to 14 km. For GABLE90, 5.2 % of the backscatter returns above 8 km were greater than 6.0×10^{-10} m^{-1} sr^{-1}. Over 53% of the backscatter values that exceeded this threshold occurred at an altitude greater than 10 km.

The relatively high frequency of backscatter returns that exceeded the thresholds used to determine cirrus clouds for the SABLE missions was not anticipated. The synoptic conditions in this region of the world would tend to inhibit cirrus formation since there are no major jet streams or major areas of convective activity in this region. Instead, the major feature is the descending branch of the Hadley cells. One possible explanation for the presence of cirrus is the convective activity over South America and the advection of cirrus generated by thunderstorms to the region of Ascension Island.

4. IMPACT OF CIRRUS ON ABL SYSTEM PERFORMANCE

The proposed ABL laser system will be on a high flying aircraft and the engagement scenarios will have long, nearly horizontal laser paths. Using the definition of optically thin cirrus employed in this study (*i.e.* a vertical optical depth less than 0.03 at 0.55 μm) a 1 km thick cloud over a range of 200 km will completely attenuate the ABL beam. Over a 100 km path, the loss would be on the order of 96%. The same system propagating vertically through a one kilometer thick cloud would be attenuated by only 3%. With these kinds of losses for long nearly horizontal paths, an examination of the impacts of cirrus on the performance of the ABL system is clearly warranted.

4.1 Engagement Scenarios

The ABL system is being designed for theater missile defense applications. Table 5 summarizes the engagement conditions for four potential threat scenarios for the ABL system. In each scenario listed, the aircraft platform is assumed to be operating at an altitude of 12.5 km.

Table 5. Potential Engagement Conditions for Four Threat Scenarios for the ABL System. In each case, the ABL platform is assumed to be at an altitude of 12.5 km

ENGAGEMENT CASE	THREAT SCENARIO	TARGET ALTITUDE	TARGET RANGE (km)
A	KOREA	15.3	320
B	IRAQ-ISRAEL	37.1	440
C	KOREA & IRAQ-ISRAEL	50.3	560
D	LIBYA-EUROPE	92.1	620

4.2 Method of Analysis

LOWTRAN7[38] was used to calculate the transmission. A tropical atmosphere with a tropopause at 16 km and background stratospheric volcanic aerosol conditions were assumed. The layers of the tropical model atmosphere were 1 km thick between 10 and 25 km. Transmission calculations for a wavelength interval from 1.31 to 1.32 μm were first done assuming no cirrus clouds for each of the four scenarios.

With the assumption that the tropopause was at 16 km, cirrus clouds were assumed to be anywhere in the 11 to 16 km altitude range. (Altitudes below the aircraft altitude had to be considered because when the effects of refraction and curvature of the atmosphere are taken into account, the laser beam could path through altitudes below the aircraft altitude under certain engagement conditions.) To simulate the effects of cirrus on the ABL system, cirrus clouds were "placed" in different altitude ranges using the LOWTRAN7 option of employing a user-specified subvisual cirrus cloud extinction coef-

[38] Kneizys, F.X., Shettle, E.P., Abreu, L.W., Chetwynd, J.H., Anderson, G.P., Gallery, W.O., Selby, J.E.A., and Clough, S.A., (1988) "Users Guide to LOWTRAN7," Air Force Geophysics Laboratory, Hanscom AFB, MA, AFGL-TR-88-0177, ADA 206773.

ficient. A cirrus cloud was first introduced in the 11 - 12 km model layer and the transmission calculated. The cirrus was then removed from that layer and placed in the next higher layer, 12-13 km, and the transmission again calculated. This procedure was repeated for the 13 - 14, 14 - 15, and 15 - 16 km model layers. In each case, the cirrus was assumed to completely fill the layer and be homogeneous through out the layer. The calculations were performed for a number of cirrus extinction coefficients (see Table 6). In all cases, the values listed in Table 6 are for a wavelength of 0.55 μm. The SABLE 88 values noted are based on an analysis of the data from all SABLE 88 missions and include all backscatter values that exceed the cirrus/no cirrus threshold, not just the values flagged as subvisual cirrus. Internally, LOWTRAN7 scales the 0.55 μm extinction values to the assumed laser wavelength of 1.32 μm. This scaling is based on assuming a subvisual cirrus cloud model with a modified gamma particle size distribution and a mode radius of 8 μm. The resulting scaling factor is 1.07.

Table 6. Cirrus Extinction Coefficients Used to Estimate the Impact of Cirrus Clouds on the ABL System. All values given are for a wavelength of 0.55 μm

Extinction Coefficient Source	Value at 0.55 μm (km^{-1})
LOWTRAN7[38]	0.03
SAGE II Analysis (Woodbury *et al.*[21])	0.004
SABLE 88 Analysis for 11 - 12 km	0.05
SABLE 88 Analysis for 12 - 13 km	0.166
SABLE 88 Analysis for 13 - 14 km	0.0003
SABLE 88 Analysis for 14 - 15 km	0.0006

4.3 Transmission Results

Figures 8, 9, 10, and 11 give the results of the transmission calculations for each engagement scenario. Each figure also includes a schematic representation of the engagement geometry of the path between the ABL system and the target. The path geometry includes the effects of refraction and curvature.

For the threat scenario of Case A, the viewing angle is 90.86° and the tangent height between the ABL system and the target is 11.77 km. Under these conditions, approximately 200 km of the 320 km path is below the altitude of the ABL system. As Figure 8 indicates, cirrus clouds impact the Case A scenario especially when the cirrus layer is below the ABL platform. This is due to the long path length (116 km) through the 10 - 11 km layer. When the cirrus is in the upper model layers, the path length decreases and the impact of cirrus on atmospheric transmission decreases. The impact is also a function of the assumed extinction coefficient for the cirrus. Similar results are found for cases B, C, and D in Figures 9, 10, and 11, respectively.

Total Path Transmission at $\lambda \approx 1.32$ μm

Cloud Layer Height (km)	$\sigma = 0.03\ km^{-1}$ *	$\sigma = 0.004\ km^{-1}$ **	SABLE88 Data
11 - 12	0.02	0.48	0.0
12 - 13	0.02	0.48	0.0
13 - 14	0.19	0.64	0.74
14 - 15	0.26	0.67	0.62
15 - 16	0.58	0.75	-
Clear Sky	0.78	-	-

* LOWTRAN7 Subvisual Cirrus at 0.55 μm
** Woodbury & McCormick SAGE Analysis for Cirrus at 0.55 μm

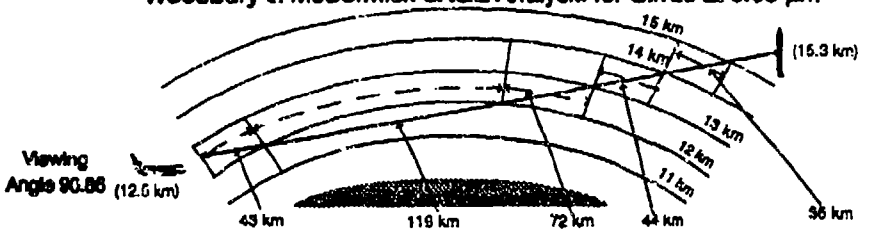

Figure 8. Comparisons of the Total Path Transmission at a Wavelength of 1.32 μm for Case A Using Three Different Assumptions for the Extinction Coefficients of Cirrus and Five Different Cirrus Layer Heights. The Extinction Coefficients for the SABLE 88 Data are Listed in Table 6.

Total Path Transmission at $\lambda = 1.32$ μm

Cloud Layer Height (km)	$\sigma = 0.03\ km^{-1}$ *	$\sigma = 0.004\ km^{-1}$ **	SABLE88 Data
11 - 12	0.86	0.86	0.86
12 - 13	0.45	0.86	0.02
13 - 14	0.29	0.79	0.83
14 - 15	0.33	0.76	0.71
15 - 16	0.37	0.77	-
Clear Sky	0.87	-	-

* LOWTRAN7 Subvisual Cirrus at 0.55 μm
** Woodbury & McCormick SAGE Analysis for Cirrus at 0.55 μm

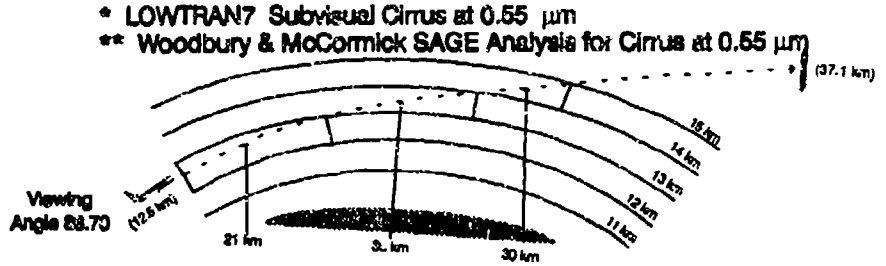

Figure 9. Comparisons of the Total Path Transmission at a Wavelength of 1.32 μm for Case B Using Three Different Assumptions for the Extinction Coefficients of Cirrus and Five Different Cirrus Layer Heights. The Extinction Coefficients for the SABLE88 Data are Listed in Table 6.

Total Path Transmission at $\lambda = 1.32\ \mu m$

Cloud Layer Height (km)	$\sigma = 0.03\ km^{-1}$ *	$\sigma = 0.004\ km^{-1}$ **	SABLE88 Data
11 - 12	0.87	0.87	0.87
12 - 13	0.48	0.87	0.02
13 - 14	0.31	0.80	0.84
14 - 15	0.35	0.76	0.72
15 - 16	0.39	0.77	-
Clear Sky	0.87	-	-

* LOWTRAN7 Subvisual Cirrus at 0.55 μm
** Woodbury & McCormick SAGE Analysis for Cirrus at 0.55 μm

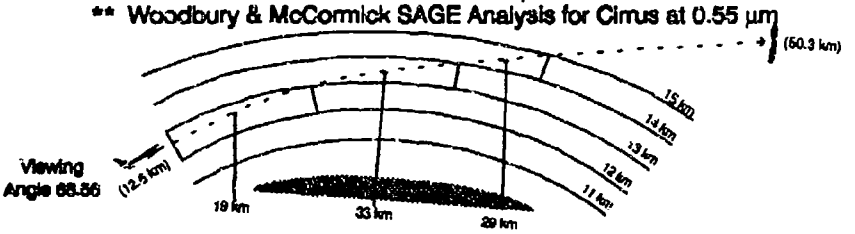

Figure 10. Comparisons of the Total Path Transmission at a Wavelength of 1.32 μm for Case C Using Three Different Assumptions for the Extinction Coefficients of Cirrus and Five Different Cirrus Layer Heights. The Extinction Coefficients for the SABLE88 Data are Listed in Table 6

Total Path Transmission at $\lambda = 1.32\ \mu m$

Cloud Layer Height (km)	$\sigma = 0.03\ km^{-1}$ *	$\sigma = 0.004\ km^{-1}$ **	SABLE88 Data
11 - 12	0.94	0.93	0.94
12 - 13	0.77	0.80	0.28
13 - 14	0.64	0.88	0.92
14 - 15	0.64	0.88	0.86
15 - 16	0.64	0.89	-
Clear Sky	0.94	-	-

* LOWTRAN7 Subvisual Cirrus at 0.55 μm
** Woodbury & McCormick SAGE Analysis for Cirrus at 0.55 μm

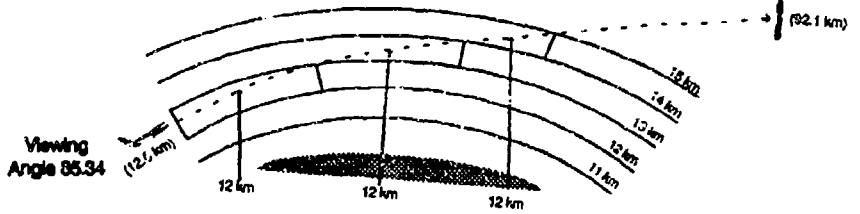

Figure 11. Comparisons of the Total Path Transmission at a Wavelength of 1.32 μm for Case D Using Three Different Assumptions for the Extinction Coefficients of Cirrus and Five Different Cirrus Layer Heights. The Extinction Coefficients for the SABLE88 Data are Listed in Table 6

4.4 Impact of the Choice of Cirrus Extinction Coefficient

The preceding figures demonstrate that the choice of assumed cirrus extinction coefficient strongly affects the total path transmission for all engagement scenarios. Figure 12 compares the LOWTRAN7 and SAGE extinction coefficients used in the analysis against those derived by Sassen *et al.*[5] from lidar measurements taken at 0.694 μm of subvisual and thin cirrus clouds. The derived extinction coefficients from Sassen *et. al.* ranged from approximately 0.008 to 0.38 km^{-1}, well above the SAGE value and generally above the LOWTRAN7 value. For comparison purposes, the range of values derived from the SABLE88 data was 0.0003 to 0.186 km^{-1}.

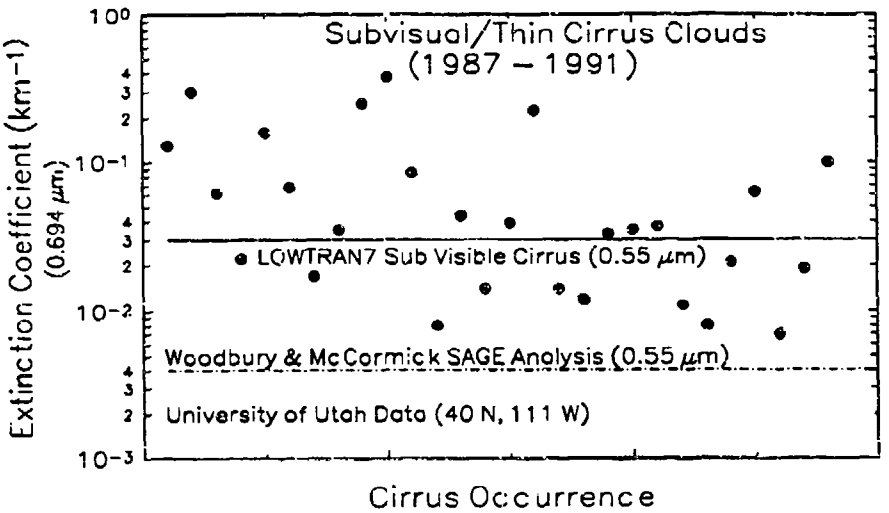

Figure 12. Comparison of SAGE and LOWTRAN7 Extinction Coefficients Against Those Inverted From Data Obtained by the University of Utah Lidar System (Sassen *et al.*[5])

The extinction coefficients obtained from both the SABLE88 analysis and the analysis of the data presented by Sassen *et al.* vary by two and one half orders of magnitude. In general, the values are greater than the values obtained from the analysis of the SAGE data while the LOWTRAN7 value used as the threshold for subvisual cirrus appears to be more representative of the values associated with subvisual cirrus presented by Sassen *et al.* Implicit in the SABLE88 and Sassen *et al.* analyses used to derive the cirrus extinction coefficients is the assumption that the ice crystals making up the cirrus clouds can be represented as spherical particles. It is noted that there are a very few models available to calculate the attenuation properties of non-spherical particles. Unfortunately, the transmission properties associated with a cirrus layer are difficult to pin down because of the natural variability of cirrus particle size, shape, number densities, etc.

4.5 Impact of Non-Homogeneity of Cirrus Clouds

Another important assumption made is that the cirrus cloud is represented as a semi-infinite homogeneous layer. It is possible to simulate a fractional cloud amount along the path between the ABL system and the target by assuming the total transmission, τ_t, is given as

$$\tau_t = \tau_a \tau_c$$

where τ_a is the clear air transmission for the entire path and the cloud transmission τ_c is given as

$$\tau_c = \exp(-\sigma_c l_i f)$$

where σ_c is the cirrus cloud extinction coefficient, l_i is the path length in the cirrus layer and f is the fraction of the path in the layer with cirrus clouds. The transmissions for the Case A scenario with an extinction coefficient of 0.03 km^{-1} and fractional cloud amounts of 1.0, 0.4, and 0.2 are given in Table 7.

Table 7. Transmission for the Case A Engagement Scenario Assuming Different Values of Fractional Cloudiness Through Cirrus Clouds

Cloud Layer (km)	Fractional Cloudiness Along Path		
	f = 1.0	f = 0.4	f = 0.2
11 - 12	0.03	0.23	0.45
12 - 13	0.03	0.23	0.45
13 - 14	0.24	0.54	0.70
14 - 15	0.32	0.60	0.74
15 - 16	0.69	0.81	0.86
Clear Sky	0.91	-	-

As the current analysis demonstrates, cirrus clouds can have an adverse effect on an ABL system, especially for the Case A engagement scenario. Assuming that the ABL platform operates at an altitude of 12.5 km, the effect of cirrus on the transmission can be reduced by engaging the target at a higher altitude. For example, for a cirrus layer between 11-12 km with an extinction coefficient of 0.03 km^{-1} the transmission for Case A is 0.02, 0.87 for Case C, and 0.94 for Case D while the respective engagement altitudes for the target is 15.3, 50.3 and 92.1 km. An alternative method is to take advantage of the fact that many of the cirrus formation mechanisms result in a banded cirrus structure that parallels the wind vector the cirrus layer is embedded in.

To investigate the influence of a structured cloud field on long path transmission for an ABL system, a fractal cloud model[39] was used to generate a cirrus cloud field for a 100 km × 100 km × 1 km volume. This model is used to produce 3-dimensional cloud

[39] Cianciola, M.E. (1992) "Cloud Scene Simulation Modeling - The Enhanced Model," TASC, Reading, MA, TASC Technical Report TR 6042-2.

fields for use in synthetic scene simulations. The horizontal resolution was 0.4 km and the vertical resolution was 50 meters. The model generates "realistic" cloud structure based on the cloud amount and cloud type for a given cloud base and thickness. Each point in the grid is flagged with a cloud liquid water (or ice) content. For the simulation presented below, a cloud amount of 40% was used. Rays parallel and perpendicular to the cloud structure were passed through the volume from each grid box at the cloud top, although rays that exited the side of the volume were removed from the analysis. The Case A viewing angle was used to determine the zenith angle of incidence of the ray relative to the cloud volume. Figure 13 shows a schematic representation of a laser beam propagating through such a cloud.

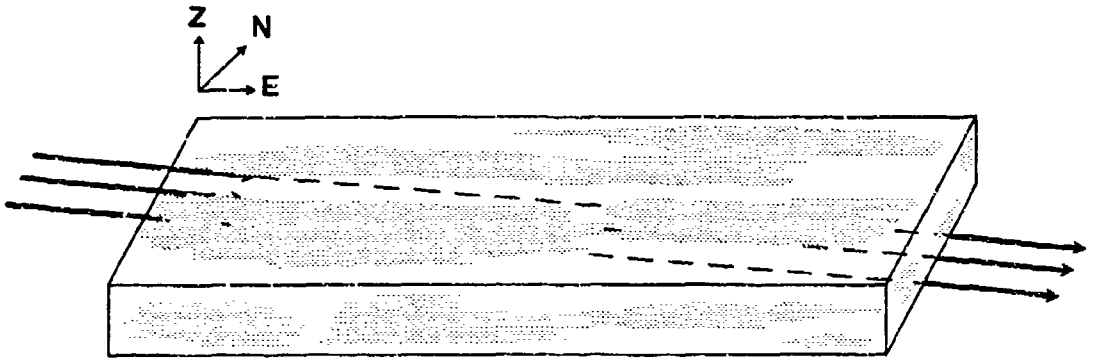

Figure 13. Schematic Representation of a Laser Beam Propagating Along a Slant Path Through a Banded Cirrus Cloud

The fractional cloud amount along each ray was determined as the number of grid boxes intersected by the ray with non-zero ice content divided by the total number of grid boxes intersected in the cloud volume. As indicated in Figure 13, the cloud structure is banded in an East-West direction; that is, a ray impinging on the volume in an East-West direction will parallel the cloud structure. The results of the analysis are given in Figure 14.

In Figure 14, 10 % of the rays in an East-West direction have a fractional cloud coverage of 0.0 while approximately 1% of the rays in a North-South direction have a cloud coverage of 0.0. This implies that there is a higher probability of having clear conditions in an East-West direction than in a North-South direction. Approximately 5 % of the rays in the East-West direction and 13 % of the North-South rays have a fractional coverage of 0.35. Finally, about 3 % of the East-West rays and less than 1 % of the North-South rays have a fractional coverage of 0.75. This implies that there is a very low probability of having a high fractional coverage (greater than 0.7) for a North-South ray. As indicated earlier, for a one kilometer thick cloud with an extinction coefficient of 0.03 km^{-1} and a cloud base at 11 km for the Case A scenario the transmission increases from 0.02 to 0.45 when the fractional cloud coverage decreases from 1.0 to 0.2. To take full advantage of the features of a structured cloud fields to optimize the performance of an ABL additional studies are required.

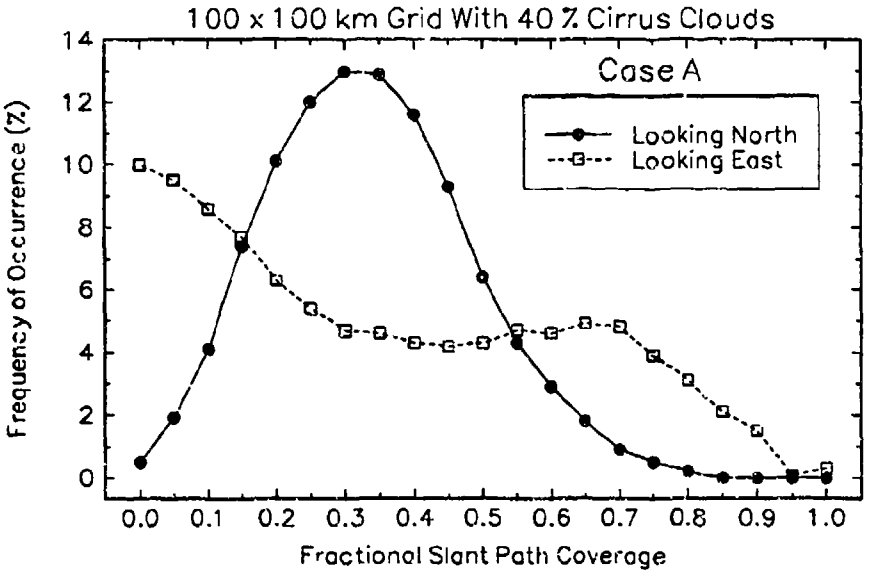

Figure 14. Frequency of Occurrence of Different Fractional Slant Path Cloud Coverage for Paths Parallel and Perpendicular to the Banded Cirrus Clouds

5. SUMMARY AND RECOMMENDATIONS FOR FUTURE WORK

5.1 Summary

The Geophysics Directorate of the USAF Phillips Laboratory is supporting efforts to estimate the environmental impacts on the proposed AirBorne Laser (ABL) system, a laser system being considered for theater missile defense. One of the environmental factors of particular concern are cirrus clouds that can be found at the proposed flight levels for the ABL system. This report presented a review of cirrus phenomenology and estimated the impact of cirrus clouds on the ABL system.

Cirrus clouds are unique because of their wide range of optical properties, they occur at high altitudes, and they tend to be more persistent than other cloud types. Because of these unique properties and because of their potential impact on climate, a number of field programs have been conducted recently to investigate the optical and microphysical properties of cirrus clouds and the mechanisms involved in cirrus formation. However, cirrus clouds are also the most difficult clouds to sense remotely from either ground-based or space-based platforms. For this reason, cirrus cloud climatologies are not as extensive or as accurate as cloud climatologies developed for other cloud types. Because of the low extinction coefficients that can be associated with cirrus clouds, these clouds can be highly transmissive for short and moderate path lengths. This is not the case for most water clouds that have fairly high extinction coefficients and low transmission for even short path lengths. The range of transmissions implies that under certain conditions the impact of cirrus clouds along the path between an ABL system and a target may not render the system inoperative.

It should not be assumed that because the ABL system will operate at an altitude above ten kilometers that it will not be affected by cirrus clouds. Certain countermeasures can be taken to reduce the impact of cirrus clouds on an ABL system. For instance, the target may be engaged at a higher altitude or, based on the cloud amount, it may be advantageous to operate the system such that the engagement path between the ABL system and the target is parallel or perpendicular to the banded structure of cirrus clouds.

5.2 Recommendations for Future Work

The investigation of the impact of cirrus clouds on the ABL system was based, in part, on measured and inverted cirrus optical properties. The spatial extent of the cirrus clouds used in this investigation was a manifestation of the model used in the simulation. That is, the cirrus cloud layer(s) are modeled as semi-infinite homogeneous layers. The influence of discontinuous cloud layers was modeled by assuming different fractional cloud cover amounts. No attempt was made to investigate the global spatial and temporal distribution of cirrus clouds. The next logical step is to assemble a cirrus spatial and temporal database from existing databases that can be used to investigate the influence of cirrus clouds on an ABL system that could be deployed any where in the world. In addition to developing databases that could be used to support ABL requirements the present models must be enhanced to accurately model the influence of fractional non homogeneous cirrus cloud amounts on long path transmission. The above review and studies of long path cirrus transmission did not address the potential effect on an ABL system of the mechanical turbulence that can occur in the vicinity of cirrus clouds, especially cirrus

clouds associated with the dynamics of the jet stream. Finally, the possibility of piggy-backing on future cirrus field programs like FIRE should be explored. These programs provide an opportunity to evaluate and validate the model simulations that have been employed to investigate the influence of cirrus EO systems.

References

1. Liou K. N., Takano,Y., Ou, S.C., A. Heymsfield, and W. Kreiss (1990) Infrared transmission through cirrus clouds: A radiative model for target detection, *Appl. Optics*, **29**:1886-1896.

2. Alejandro, S.B., Koenig, G.G., Vaughan, J.M. and Davies, P.H. (1990) SABLE: A South Atlantic aerosol backscatter measurement program, *Bull. Amer. Meteor. Soc.*, **71**:281-287.

3. Heymsfield A. J. and C. M. R. Platt, C.M.R. (1984) A parameterization of particle size spectrum of ice clouds in terms of the ambient temperature and the ice water content, *J. Atmos Sci.*, **41**:846-855

4. Liou, K.N., (1986) Influence of cirrus clouds on weather and climate processes: A global perspective, *Mon. Wea. Rev.*, **114**:1167-1197.

5. Sassen K. and Cho, B.S. (1992) Subvisual-Thin Cirrus Lidar Dataset for Satellite Verification and Climatological Research, *J. Appl. Meteor.*, **31**:1275-1285.

6. Schiffer R.A. and Rossow, W.B.(1983) The International Satellite Cloud Climatology Project (ISCCP): The first project of the world climate research programme, *Bull. Amer. Meteor. Soc.*, **64**:2682-2694.

7. Cox, S.K., McDougal, D.S., Randall, D.A., and Schiffer, R.A. (1987) FIRE-The First ISCCP Regional Experiment, *Bull. Amer. Meteor. Soc.*, **68**:114-118.

8. WCRP-14 (1988) "An Experimental Cloud Lidar Pilot Study (ECLIPS), report of the WCRP/CSIRO workshop on cloud base measurement, CSIRO, Mordialloc, Victoria, Australia, 29 February - 3 March 1988, WMO/TD-No. 251.

9. Ackerman, S.A., Eloranta, E.W., Grund, C.J., Knuteson, R.O., Revercomb, H.E., Smith,W.L., and Wylie, D.P. (1993) University of Wisconsin cirrus remote sensing pilot experiment, *Bull. Amer. Meteor. Soc.*, **74**:1041-1049.

10. Oltmans, S.J., (1986) "Water vapor profiles for Washington, DC; Boulder, CO; Palestine, TX; Laramie, WY; and Fairbanks, AK; during the period 1947 to 1985, NOAA Data Rep. ERL-ARL-7.

11. London, J., (1957) "A study of the atmospheric heat balance. Final Rep.,": Contract AF19(122)-165, Dept. of Meteor. and Oceanogr., New York University, 99 pp. (ASTIA 117 227 Air Force Geophysics Laboratory, Hanscom AFB, MA. 01730.)

12. Hahn, C.J., Warren, S.G., London, J., Chervin R.M., and Jenne, R. (1982) Atlas of Simultaneous Occurrence of Different Cloud Types over the Ocean. NCAR/TN-201+STR, National Center for Atmospheric Research, 212 pp.

13. Fye, F.K., (1978) "The AFGWC automated cloud analysis model," Tech. Memo. 78-002, Air Force Global Weather Central, Offut Air Force Base, NE, 97 pp.

14. Rossow, W.B., and Lucis, A.A. (1990) Global seasonal cloud variations from satellite radiance measurements part II: Cloud properrties and radiative effects, *J. Climate*, **3**:1204-1253.

15. Rossow, W.B., and Schiffer, R.A. (1991) International satellite cloud climate project products, *Bull. Amer. Meteor. Soc.*, **2**.

16. Stowe, L.L., Yeh, H.Y.M, Eck, T.F., Wellemeyer, G.G., Kyle, H.L,. and the NIMBUS-7 cloud data processing team (1989) Nimbus-7 global cloud climatology part II: First year results, *J Climate*, **2**:671-709.

17. Barton, I.J. (1983) Upper level cloud climatology from an orbiting satellite, J. Atmos. Sci., 40:435-447.

18. Menzel, W.P., Wylie, D.P., and Strabala, K.I. (1992) Seasonal and diurnal changes in cirrus clouds as seen in four years observations with the VAS, *J. Appl. Meteor.*, **31**:370-384.

19. Grund, C.J., and Wylie, D. (1989) Lidar validations of VAS; cirrus cloud height determinations. AIAA paper 89-0804, 27th Aerospace Sciences Meeting, January 9-21, Reno, Nevada.

20. Woodbury, G.E., and McCormick, M.P. (1986) Zonal and geographical distributions of cirrus clouds determined from SAGE data, *J. Geophy. Res.*, **91**:2775-2785.

21. Liou, K.N., Ou, S.C. and Koenig, G.G. (1990) "An investigation on the climate effect of contrail cirrus", Lecture Notes in Engineering Air Traffic & Environment: Background Tendency and Potential Global Atmospheric Effects, Ed U. Schumann, Springer-Verlag.

22. Changnon, S. A. Jr., (1981) Midwestern cloud, sunshine, and temperature trends since 1961: Possible evidence of jet contrail effects, *J. Appl. Meteor.*, **20**:496-508.

23. Conover, J., (1960) Cirrus patterns and related air motions near the jet stream as derived by photography, *J. Meteor.*, **17**:532-546.

24. Heymsfield, A.J., (1975) Cirrus uncinus generating cells and the evolution of cirriform clouds. Part I: Aircraft observations of the growth of the ice phase, *J. Atmos. Sci.*, **32**:799-808.

25. Heymsfield, A.J., (1975) Cirrus uncinus generating cells and the evolution of cirriform clouds. Part II: The structure and circulations of the cirrus uncinus generating head, *J. Atmos. Sci.*, **32**:809-819.

26. Heymsfield, A.J., (1975) Cirrus uncinus generating cells and the evolution of cirriform clouds. Part III: Numerical computations of the growth of the ice phase, *J. Atmos. Sci.*, **32**:820-830.

27. Starr, D.O., and Cox, S.K. (1985) Cirrus clouds. Part II: Numerical experiments on the formation and maintenance of cirrus, *J. Atmos. Sci.*, **42**:2682-2694.

28. Platt, C.M.R., Scott, J.C., and Dilley, A.C. (1987) Remote sounding of high clouds. Part VI: Optical properties of midlatitude and tropical cirrus, *J. Atmos. Sci.*, **44**:729-747.

29. Minnis, P., Young, D.F., Sassen, K., Alvarez, J.M. and Grund, C.J. (1990) The 27-28 October 1986 FIRE IFO cirrus case study: Cirrus parameter relationships derived from satellite and lidar data," *Mon. Wea. Rev.*, **118**:2426-2446.

30. Spinhirne, J.D. and Hart, W.D. (1990) Cirrus structure and radiative parameters from airborne lidar and spectral radiometer observations: The 28 October 1986 FIRE study, *Mon. Wea. Rev.*, **118**:2329-2343.

31. Wielicki, B.A., Suttles, J.T., Heymsfield, A.J., Welch, R.W., Spinhirne, J.D., Wu, M.L.C., Starr, D.O., Parker, L,. and Ardnini, R.F. (1990) The 27-28 October 1986 FIRE IFO cirrus case study: Comparison of radiative transfer theory with observations by satellite and aircraft, *Mon. Wea. Rev.*, **118**:2356-2376.

32. Sassen, K., Heymsfield, A.J., and Starr, D.O. (1991) "Is there a cirrus small particle radiative anomaly?" preprint 7th conference on Atmospheric Radiation, July 23-27 1990, San Francisco, CA. J91-J95.

33. Muinonen, K., (1989) Scattering of light by crystals: a modified Kirchoff approximation, *Appl. Opt.*, **28**: 3044-3049.

34. Woodfield, A.A. and Vaughn, J.M. (1983) Airspeed and wind shear measurements with an airborne CO_2 CW laser, *Int. J. Aviation Safety*, **2**:207-224.

35. Rogers, R.R (1979) Chapter 8 "Formation and Growth of Ice Crystals" in A Short Course in Cloud Physics, Second Edition, Pergamon Press International, New York, NY.

36. Anderson, G.P., Clough, S.A., Kneizys, F.X., Chetwynd, J.H., and Shettle, E.P. (1986) "AFGL Atmospheric Constituent Profiles (0 - 120 km)", Air Force Geophysics Laboratory, Hanscom AFB, MA, AFGL-TR-86-0110, 15 May, ADA 175173.

37. Longtin, D.R., Koenig, G.G., Hummel, J.R., and Jones, J.R. (1993) "Analysis of Aircraft-Based Lidar Backscatter Measurements from the SABLE and GABLE Programs," Phillip Laboratory, Hanscom AFB, MA, PL-TR-93-2026.

38. Kneizys, F.X., Shettle, E.P., Abreu, L.W., Chetwynd, J.H., Anderson, G.P., Gallery, W.O., Selby, J.E.A., and Clough, S.A., (1988) "Users Guide to LOWTRAN7," Air Force Geophysics Laboratory, Hanscom AFB, MA, AFGL-TR-88-0177, ADA 206773.

39. Cianciola, M.E. (1992) "Cloud Scene Simulation Modeling - The Enhanced Model," TASC, Reading, MA, TASC Technical Report TR 6042-2.